Optical Generation of Hot Spin-Polarized Electrons from a Ferromagnetic Two-Dimensional Electron Gas

Martin Ellguth,[1,*] Christian Tusche,[1] and Jürgen Kirschner[1,2]
[1]Max-Planck-Institut für Mikrostrukturphysik, Weinberg 2, 06120 Halle, Germany
[2]Institut für Physik, Martin-Luther-Universität Halle-Wittenberg, 06120 Halle, Germany
(Received 3 September 2015; revised manuscript received 2 November 2015; published 23 December 2015)

Linearly polarized light with an energy of 3.1 eV has been used to excite highly spin-polarized electrons in an ultrathin film of face-centered-tetragonal cobalt to majority-spin quantum well states (QWS) derived from an sp band at the border of the Brillouin zone. The spin-selective excitation process has been studied by spin- and momentum-resolved two-photon photoemission. Analyzing the photoemission patterns in two-dimensional momentum planes, we find that the optically driven transition from the valence band to the QWS acts almost exclusively on majority-spin electrons. The mechanism providing the high spin polarization is discussed by the help of a density-functional theory calculation. Additionally, a sizable effect of spin-orbit coupling for the QWS is evidenced.

DOI: 10.1103/PhysRevLett.115.266801 PACS numbers: 73.21.Fg, 79.60.Bm

The spin of electrons is strongly considered as the carrier of information in future electronic devices categorized as spintronics [1,2]. Nowadays, sophisticated means exist to efficiently measure spin-polarized electron currents in vacuum [3] or in solids [4]. Their generation in vacuum has been realized by spin-polarized electron guns enabling experiments such as spin-polarized electron energy loss spectroscopy [5,6] and spin-polarized inverse photoemission [7,8]. For spintronics, a prerequisite is the injection of spin-polarized currents into a semiconductor. Since the feasibility of using drift currents for this purpose has been disproved due to the much lower conductance of semiconductors compared to ferromagnetic metals [9], diffusion of spin-polarized, hot electrons [10] across a potential barrier is an important alternative [11,12]. Specifically, for cobalt thin films as a source of polarized electrons, an example of diffusion-driven injection into an organic semiconductor is reported in [13].

In this work, we concentrate on the optically excited interband transition in face-centered-tetragonal (fct) cobalt thin films which allows for generating highly spin-polarized, hot electrons below the vacuum level as demonstrated in [13,14]. In two-photon photoemission (2PPE) measurements, this transition occurs as the first (*pump*) step of a resonant two-photon (*pump-probe*) process, exciting a valence-band (VB) electron to an unoccupied sp band. Confinement of electrons to the few-monolayer thin Co film transforms the sp band to quantum well states (QWS) with discrete $k_\perp$ values. The pump-probe process schematically reads VB $\rightarrow$ QWS $\rightarrow e^-$, where each arrow represents one photon, and e^- is the photoelectron whose spin is measured to draw conclusions about the spin selectivity of the VB $\rightarrow$ QWS step. Going beyond the normal-emission 2PPE results in [13,14], we measure the spin polarization for a broader range of electronic states, including those with nonzero in-plane Bloch wave vector components, which take part in the diffusive injection of spin-polarized currents from cobalt thin films and thus play an important role in view of spintronics devices. With the QWS situated approximately 3 eV above the Fermi level, we propose that the spin-selective excitation process VB $\rightarrow$ QWS may be used in a semiconductor-metal heterostructure where the junction could be designed to provide a potential barrier that acts as a high-pass energy filter for hot electrons.

Experimentally, we used spin-resolved photoelectron *momentum microscopy* [15,16] as an efficient, parallelized alternative to scanning angle-resolved photoemission, capturing every photoelectron in one shot without any limitation of the acceptance angle. The spin polarization of each beam forming the electron-optical image was detected simultaneously by specular reflection from a $W(100)$ surface using the (00) LEED spot, exploiting spin-orbit coupling for a spin-dependent scattering probability. Within the spin-resolved momentum images obtained by this technique, an unambiguous separation of the resonant process VB $\rightarrow$ QWS $\rightarrow e^-$ from the nonresonant process VB $\rightarrow\!\rightarrow e^-$ became possible for the first time and revealed *nearly perfect* spin filtering as opposed to only moderate enhancement of the spin polarization which was previously believed. For 2PPE experiments, the second harmonic of a home-built, mode-locked Ti:sapphire oscillator was used yielding 20 fs pulses with a central photon energy of 3.1 eV [17]. Pseudomorphic cobalt thin films were grown on Cu(001) resulting in a fct structure with lattice constants $a = 3.61$ Å (in plane) and $c = 3.47$ Å (perpendicular) [18].

To visualize the region within k space that is probed in our experiments, Fig. 1 shows the Brillouin zone and the band structure of bulk fct cobalt calculated by density functional theory using the local spin density

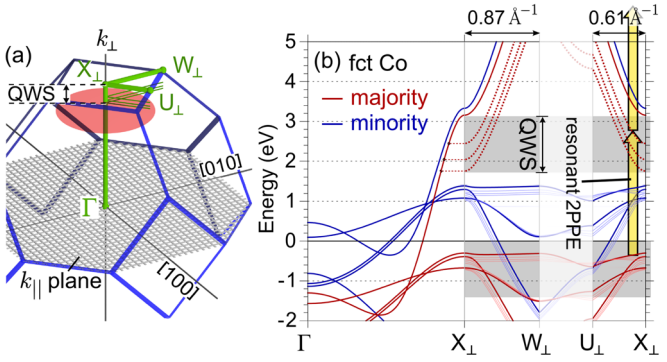

FIG. 1 (color online). (a) fct Brillouin zone; the high-symmetry axes used in (b) are marked by green rods. The red disk approximately corresponds to the k-space region, where QWS are probed in our momentum-resolved 2PPE experiments. The high-symmetry points on the top are written with index ($\perp$), to distinguish them from the inequivalent points at the sides. (b) density-functional-theory–local-spin-density-approximation calculation of fct cobalt. Regions highlighted in gray indicate the energy ranges of initial and intermediate states involved in our 2PPE experiments. Dashed and thin-line curves are calculated along vertically shifted $\overline{X_\perp W_\perp}$ and $\overline{X_\perp U_\perp}$ axes as indicated in (a). In the case of the sp band, only the majority spin is shown for clarity.

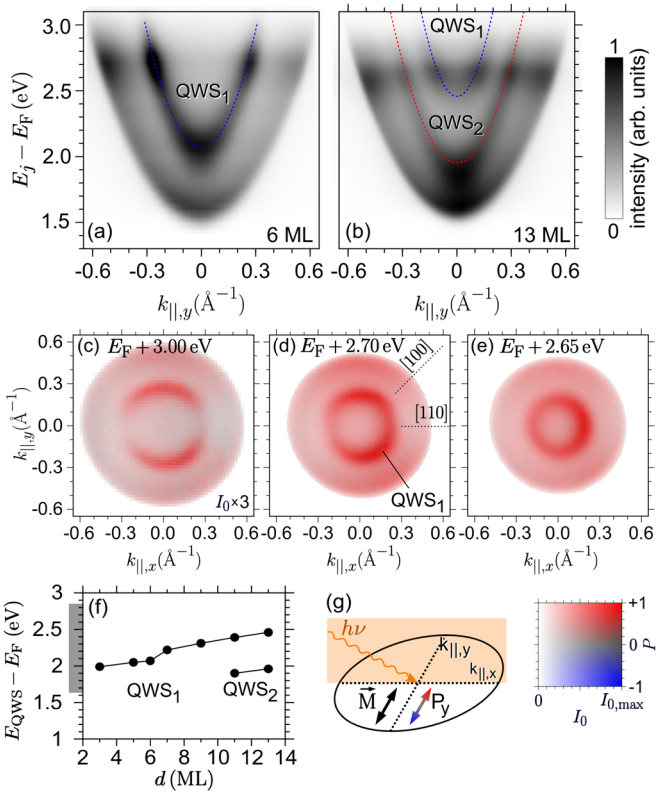

FIG. 2 (color online). Two-photon photoemission of cobalt thin films on Cu(001) using p-polarized laser radiation ($h\nu = 3.1$ eV); (a), (b) $I(k_{\parallel,y}, E)$ spectra for 6 and 13 monolayers of cobalt. E_j denotes the energy of the intermediate state after the pump step. (c)–(e) spin-resolved $I(k_{\parallel,x}, k_{\parallel,y})$ spectra for six monolayers of cobalt at intermediate state energies indicated in the graphs. (f) Energies of the QWS parabola minima for a series of cobalt overlayer thicknesses. (g) Photoemission geometry.

approximation [19,20]. Using momentum microscopy, we probe an area in k space that is schematically indicated by the red disk in Fig. 1(a), while standard photoemission in normal emission would only probe the center of such a disk. The vertical position, or the range of $k_\perp$ values that contributes to the photoemission current, is usually implicitly determined by the photon energy. When observing photoemission from QWS, however, the involved $k_\perp$ is additionally selected by the $k_\perp$ discretization of the QWS. By tuning the film thickness, $k_\perp$ can be selected within a range indicated in Fig. 1(a), where the Co sp band and the projected band gap of Cu(100) coincide [21]. As easily recognized, the probed k space includes regions beyond the high-symmetry axes usually shown in band structure plots. In our calculation, we included two axes spanning the $k_\parallel$ plane and show how the dispersion changes when shifting these axes towards the center of the Brillouin zone [dashed lines in Fig. 1(b)], giving an approximate description of the experimentally probed k region. A resonant 2PPE process VB → QWS → e^- is indicated in Fig. 1(b). One photon resonantly excites an electron to a QWS and the second photon excites this electron further to energies above the vacuum level.

Figure 2 shows two-photon photoemission measurements of Co thin films on Cu(001), performed for a range of thicknesses from 3 to 13 monolayers [22]. $I(k_{\parallel,y}, E)$ spectra reveal the quasi-free-electron–like dispersion of the quantum well state(s), characterizing these electronic states as a two-dimensional electron gas confined to the Co thin film. The experimentally observed dispersion in Figs. 2(a) and 2(b) compares favorably to the dispersion shown in Fig. 1(b) along $\overline{X_\perp W_\perp}$. With increasing film thickness, the number of allowed, discretized $k_\perp$ values increases, and more than one QWS is present (11 and 13 monolayers). The continuously varying dependence of the QWS energy on film thickness, shown in Fig. 2(f), allows us to establish the connection between QWS$_1$ in Fig. 2(a) and QWS$_1$ in Fig. 2(b). The energetic shift of each QWS with increasing thickness deviates from the textbook example of a flat-potential quantum well, since it is governed mostly by the crystal potential as also observed in earlier studies [23,24]. A quantitative characterization of the dispersion seen in Figs. 2(a) and 2(b) is provided in the Supplemental Material [25].

Figures 2(c)–2(e) are spin-resolved momentum images measured at three energies with a photoemission geometry as indicated in Fig. 2(g). The sample was remanently magnetized along the y axis, parallel to the spin-sensitive axis of the detector. The azimuth of the incident, p-polarized laser pulses was along the x axis. The combined

information of intensity and spin polarization is expressed by the two-dimensional color code showing spin-up (spin-down) intensity as saturated red (blue), unpolarized intensity as gray and zero intensity as white. At all measured energies, the photoemission current is dominated by majority-spin electrons (red color). Within the ringlike regions, the excitation of photoelectrons proceeds resonantly via the QWS as an intermediate state, and the spin polarization reaches maximum values which are between +60% and +80% in Figs. 2(c)–2(e). Earlier works have reported values of 51% [13], or 46% [14] in normal emission geometry. Since these spin polarization values represent a weighted average of resonant 2PPE via the QWS and nonresonant 2PPE, the intensity of the QWS peak itself influences this overall spin polarization. In that sense, our findings are consistent with these earlier experiments. The azimuthal intensity variation of the QWS-related photoemission intensity (high intensity along $k_{\parallel,y}$ and low intensity along $k_{\parallel,x}$) is an effect of the non-normal incidence of light, reducing the fourfold rotational symmetry of the sample to a mirror symmetry when considering the complete photoemission geometry. In the remaining $k_{\parallel}$ area, *nonresonant transitions* exciting the photoelectron directly from the VB occur with both lower intensity and lower spin polarization values in the range from +30% to +70%.

In Fig. 3, we use the partial-intensity representation $I_{\uparrow,\downarrow} = (I/2)(1 \pm P)$ of the data in Fig. 2(c), where I is the spin-integral intensity and P is the spin polarization. Here, spin-up ($I_{\uparrow}$) corresponds to majority spin. We find that not only is the QWS feature dominant in the majority-spin channel, but it is also completely absent in the minority-spin channel. The intensity in the minority channel consists only of a homogeneous background of nonresonant transitions (VB $\rightarrow\rightarrow e^-$). This strikingly pure spin-up character of the QWS photoemission feature requires that the first step (VB $\rightarrow$ QWS) of the resonant two-photon process (VB $\rightarrow$ QWS $\rightarrow e^-$) must proceed with a selectivity for majority spin close to 100%—a conclusion that became possible only by employing spin-resolved momentum microscopy, since earlier normal photoemission experiments did not allow for an unambiguous separation of the QWS peak from the intensity background of nonresonant transitions.

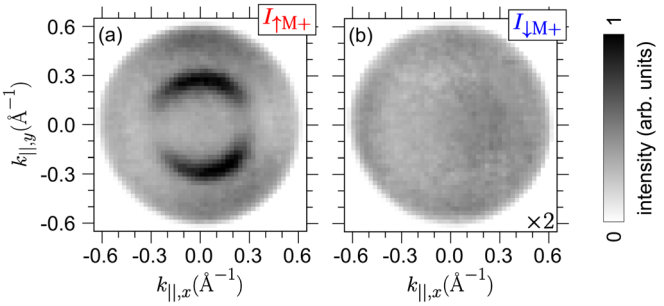

FIG. 3 (color online). Spin-up (a) and spin-down (b) partial intensities of the two-photon photoemission process for six monolayers of cobalt on Cu(001) remanently magnetized in the $M+$ direction at an intermediate state energy $E_F + 3.0$ eV.

Interestingly, the incidence of the laser pulses and their orientation relative to the magnetization vector has an effect on the degree of spin polarization for resonant excitations of the QWS, as is shown in the following.

In Figs. 4(a) and 4(b), the magnetization of the sample has been reversed with respect to the measurement in Fig. 3. The primary effect in a ferromagnet with an exchange-split band structure is that the lower-energetic majority-spin states and higher-energetic minority-spin states are defined with respect to the magnetization. When reversing the magnetization, majority spin and minority spin, measured as spin-up and spin-down in a laboratory frame, switch their roles. Consequently, the measured spin polarization changes its sign. Indeed, we find $I_{\uparrow,M+} \approx I_{\downarrow,M-}$ for the majority spin channel with the strong QWS resonance.

However, a second, contrary effect arises due to spin-orbit interaction, which manifests itself in the nonvanishing signature of the QWS in the minority spin channel for $M-$ ($I_{\downarrow,M+} \neq I_{\uparrow,M-}$). In terms of the spin polarization, this behavior can be expressed by $P_{M+} \neq -P_{M-}$. It is well known that on nonmagnetic, cubic (001) surfaces, linearly polarized light excites spin-polarized photoelectrons [26]. In magnetic materials, this effect adds a contribution to the spin polarization which does not depend on the magnetization direction. The interplay of exchange splitting and

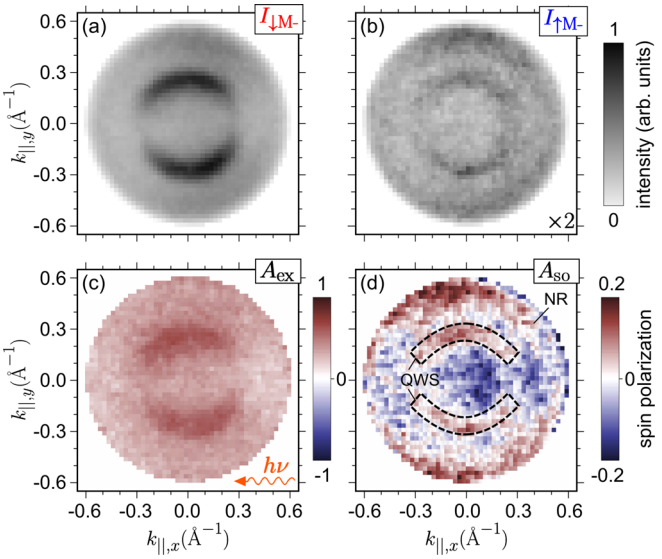

FIG. 4 (color online). (a), (b) Spin-up and spin-down partial intensities obtained in two-photon photoemission from six monolayers of cobalt on Cu(001), remanently magnetized in the $M-$ direction at an intermediate state energy $E_F + 3.0$ eV. (c), (d) exchange (A_{ex}) and spin-orbit (A_{SO}) contribution to the spin polarization.

spin-orbit interaction is furthermore known as the origin of magnetic dichroism which has been previously observed in cobalt [27,28].

From the partial intensities obtained for each of the magnetizations we calculate the following asymmetries, which separate the (nonmagnetic) contribution of the spin-orbit interaction (A_{SO}) from the exchange interaction (A_{ex}) [29] to the spin polarization.

$$A_{\mathrm{SO}} = \frac{I_{\uparrow,M+} - I_{\downarrow,M+} + I_{\uparrow,M-} - I_{\downarrow,M-}}{I_{\uparrow,M+} + I_{\downarrow,M+} + I_{\uparrow,M-} + I_{\downarrow,M-}}, \quad (1)$$

$$A_{\mathrm{ex}} = \frac{I_{\uparrow,M+} - I_{\downarrow,M+} - I_{\uparrow,M-} + I_{\downarrow,M-}}{I_{\uparrow,M+} + I_{\downarrow,M+} + I_{\uparrow,M-} + I_{\downarrow,M-}}. \quad (2)$$

Figures 4(c) and 4(d) show the resulting $A_{\mathrm{ex}}(k_{\parallel,x}, k_{\parallel,y})$ and $A_{\mathrm{SO}}(k_{\parallel,x}, k_{\parallel,y})$ The exchange contribution A_{ex} to the spin polarization strongly outweighs the spin-orbit contribution (in the order of 10%), consistent with the common understanding that spin-orbit interaction is a comparably small effect in the ferromagnetic $3d$ transition metals. The positive sign of A_{ex} is due to the majority band from where electrons are excited. In the case of A_{SO}, the sign depends on the details of the spin-orbit hybridized wave functions for each of the electronic states involved in the photoemission process and requires an in-depth theoretical analysis. Since the photoemission geometry in our experiments combines non-normal incidence of light and mostly non-normal emission, (nonmagnetic) spin polarization contributions are in principle allowed for most of the k points, other than the classical cases discussed for higher-symmetric photoemission setups [26,30]. Symmetry considerations adapted to our photoemission geometry (regarding horizontal and vertical mirror operations and rotation around $k_{\perp}$ by 180°) impose only one restriction: $A_{\mathrm{SO}}(k_{\parallel,x}, k_{\parallel,y}) = A_{\mathrm{SO}}(k_{\parallel,x}, -k_{\parallel,y})$, which is directly confirmed by our data. The quantitative characterization of A_{SO} directly visualizes different spin-orbit contributions of the process VB → QWS → e^- compared to the process VB →→ e^-. In the Supplemental Material [25], we present the analysis of the same experiment performed with s-polarized instead of p-polarized irradiation, where the A_{SO} contribution is much smaller.

We refer again to Fig. 1(b) for a discussion of the high spin selectivity which we observed in the resonant two-photon processes (VB → QWS → e^-). The exchange splitting between majority and minority QWS is 0.2 eV in agreement with experimental results from inverse photoemission [8]. Hence, in principle, QWS of both spins are within the range of energies covered by our 2PPE experiments. Since the QWS are initially unoccupied, an electron has to be provided by excitation from the valence bands. In the relevant range of energies and momenta (lower gray-shaded area), an almost flat, nondispersive majority-spin d band exists. The flatness is favorable for providing a vertical transition (with an energy difference of $h\nu = 3.1$ eV) to the majority-spin QWS. The only minority-spin states occur for $k_{\parallel}$ radii greater than 0.3 Å^{-1} (at $E_F = 0$ along $\overline{X_{\perp}U_{\perp}}$ and $\overline{X_{\perp}W_{\perp}}$) and these exhibit a relatively steep dispersion corresponding to a low density of states. Therefore, electronic states which may serve for the direct excitation to minority-spin QWS are rare or absent within a range $0 < |k_{\parallel}| < 0.3$ Å.

Considering the valence electronic states as plotted in Fig. 1(b), it is rather surprising that our experiments showed an almost uniform intensity of the QWS resonance in Fig. 2(a). It is well known that Co hosts a strongly correlated electron system and recent calculations that incorporate the correlation effects [31], suggest a particularly strong energy broadening of majority quasiparticle bands for energies $E < E_F$. Thus, majority electrons with a rather broad-peaked density of states act as a reservoir for the pump step, explaining the low intensity variation. The absence of the minority QWS in our spectra, besides the reason given so far, can be further explained by (1) sharp minority spin quasiparticle bands at $E < E_F$, which impose stricter criteria on the resonance condition of the pump step and (2) broadened minority quasiparticles at energies $E > E_F$ which lower the transition probability for an excitation to the minority-spin QWS.

We note that the high spin selectivity in the 2PPE experiments shown here can be circumvented, e.g., if one is interested in the detection of the minority QWS, as has been demonstrated by spin-resolved inverse photoemission experiments [8]. In such experiments, electrons are provided as LEED states—free electrons that couple to bulk states or evanescent states inside the sample, which are then deexcited to the unoccupied QWS. By irradiating the sample with either spin-up or spin-down electrons, the sensitivity to the respective spin can be tuned by experiment other than in 2PPE, where the spin of electrons available for pumping to the QWS is determined by electronic states in the valence bands.

Regarding the injection of spin-polarized currents for spintronics applications, two additional effects need to be considered. (1) Electrons excited to energies from E_F to $E_F + 1.5$ eV—although not accessible in our 2PPE experiments—are expected to be dominantly of minority spin according to Fig. 1(b). A device structure that will exploit the injection of highly spin-polarized electrons from the QWS has to be designed in a way that these electrons will be filtered by a suitable choice of the potential barrier, e.g., by a Schottky contact. (2) To estimate the mean free path of majority-spin electrons, we refer to time- and spin-resolved two-photon photoemission experiments that have shown lifetimes of 8 fs for majority electrons at energies $E_F +$ 1 eV and a factor of 1.7 lower for minority electrons [32]. Extrapolating the energy dependence, a lifetime of at least 2 to 5 fs is expected for majority electrons up to $E_F + 3$ eV. The group velocity in the upper gray-shaded energy range

in Fig. 1(b) reaches up to $8/\hbar$ eV/Å^{-1} resulting in a mean free path in the range of 24 to 60 Å, or 14 to 34 monolayers.

The present results show that irradiation of a fct Co(001) surface with linearly p-polarized light ($h\nu = 3.1$ eV) leads to an almost purely majority-spin polarized ensemble of hot electrons in the QWS for the geometry chosen according to Fig. 2(g) and energies $E > E_F + 1.5$ eV. By calculating the band structure including relevant low-symmetry axes, we explained why this holds even for non-normal emission directions. The high spin polarization achieved in the pump step is a joint result of exchange splitting in the band structure of the ferromagnetic cobalt, an interband transition that suppresses minority electrons, spin-orbit coupling, and correlation effects.

M. E. acknowledges support from the BMBF (Grant No. 05K12EF1).

*mellguth@mpi-halle.de

[1] S. A. Wolf, D. D. Awschalom, R. A. Buhrman, J. M. Daughton, S. von Molnár, M. L. Roukes, A. Y. Chtchelkanova, and D. M. Treger, Science **294**, 1488 (2001).
[2] I. Źutic, J. Fabian, and S. Sarma, Rev. Mod. Phys. **76**, 323 (2004).
[3] C. Tusche, M. Ellguth, A. Krasyuk, A. Winkelmann, D. Kutnyakhov, P. Lushchyk, K. Medjanik, G. Schönhense, and J. Kirschner, Ultramicroscopy **130**, 70 (2013).
[4] D. Hägele, M. Oestreich, W. W. Rühle, N. Nestle, and K. Eberl, Appl. Phys. Lett. **73**, 1580 (1998).
[5] R. Vollmer, M. Etzkorn, P. S. Anil Kumar, H. Ibach, and J. Kirschner, Phys. Rev. Lett. **91**, 147201 (2003).
[6] D. L. Abraham and H. Hopster, Phys. Rev. Lett. **62**, 1157 (1989).
[7] J. Unguris, A. Seiler, R. J. Celotta, D. T. Pierce, P. D. Johnson, and N. V. Smith, Phys. Rev. Lett. **49**, 1047 (1982).
[8] D. H. Yu, M. Donath, J. Braun, and G. Rangelov, Phys. Rev. B **68**, 155415 (2003).
[9] G. Schmidt, D. Ferrand, L. W. Molenkamp, A. T. Filip, and B. J. van Wees, Phys. Rev. B **62**, R4790 (2000).
[10] Electrons with a higher kinetic energy than in thermal equilibrium.
[11] Y. Ando, K. Hamaya, K. Kasahara, Y. Kishi, K. Ueda, K. Sawano, T. Sadoh, and M. Miyao, Appl. Phys. Lett. **94**, 182105 (2009).
[12] I. Appelbaum, Phil. Trans. R. Soc. A **369**, 3554 (2011).
[13] M. Cinchetti, K. Heimer, J.-P. Wüstenberg, O. Andreyev, M. Bauer, S. Lach, C. Ziegler, Y. Gao, and M. Aeschlimann, Nat. Mater. **8**, 115 (2009).
[14] C.-T. Chiang, A. Winkelmann, J. Henk, F. Bisio, and J. Kirschner, Phys. Rev. B **85**, 165137 (2012).
[15] B. Krömker, M. Escher, D. Funnemann, D. Hartung, H. Engelhard, and J. Kirschner, Rev. Sci. Instrum. **79**, 053702 (2008).
[16] C. Tusche, M. Ellguth, A. A. Ünal, C.-T. Chiang, A. Winkelmann, A. Krasyuk, M. Hahn, G. Schönhense, and J. Kirschner, Appl. Phys. Lett. **99**, 032505 (2011).
[17] F. Bisio, M. Nývlt, J. Franta, H. Petek, and J. Kirschner, Phys. Rev. Lett. **96**, 087601 (2006).
[18] E. Navas, P. Schuster, C. Schneider, J. Kirschner, A. Cebollada, C. Ocal, R. Miranda, J. Cerdá, and P. de Andrés, J. Magn. Magn. Mater. **121**, 65 (1993).
[19] J. P. Perdew and Y. Wang, Phys. Rev. B **45**, 13244 (1992).
[20] All-electron full-potential linearised augmented-plane wave (FP-LAPW) code, http://elk.sourceforge.net/.
[21] Strictly, the red disk is an approximation to a curved manifold. The $k_\perp(k_\parallel)$ dependence arises because, as follows from the phase accumulation model [24], the quantization condition for $k_\perp$ contains the projected band-gap edges of substrate and overlayer, which both depend on $k_\parallel$.
[22] Thicknesses have been calibrated by medium energy electron diffraction (MEED).
[23] C.-T. Chiang, A. Winkelmann, P. Yu, J. Kirschner, and J. Henk, Phys. Rev. B **81**, 115130 (2010).
[24] M. Milun, P. Pervan, and D. P. Woodruff, Rep. Prog. Phys. **65**, 99 (2002).
[25] See Supplemental Material at http://link.aps.org/supplemental/10.1103/PhysRevLett.115.266801 for a quantitative analysis separating the spin polarization related to the QWS from the non-resonant transitions, additional experimental data using s-polarized light, and a quantitative analysis of the $k_\parallel$ dispersion.
[26] E. Tamura and R. Feder, Europhys. Lett. **16**, 695 (1991).
[27] A. Fanelsa, E. Kisker, J. Henk, and R. Feder, Phys. Rev. B **54**, 2922 (1996).
[28] D. Venus, W. Kuch, M.-T. Lin, C. M. Schneider, H. Ebert, and J. Kirschner, Phys. Rev. B **55**, 2594 (1997).
[29] J. Henk, J. Phys. Condens. Matter **13**, 833 (2001).
[30] J. Henk, T. Scheunemann, and R. Feder, J. Phys. Condens. Matter **9**, 2963 (1997).
[31] J. Sánchez-Barriga, J. Braun, J. Minár, I. Di Marco, A. Varykhalov, O. Rader, V. Boni, V. Bellini, F. Manghi, H. Ebert, M. I. Katsnelson, A. I. Lichtenstein, O. Eriksson, W. Eberhardt, H. A. Dürr, and J. Fink, Phys. Rev. B **85**, 205109 (2012).
[32] M. Aeschlimann, M. Bauer, S. Pawlik, W. Weber, R. Burgermeister, D. Oberli, and H. Siegmann, Phys. Rev. Lett. **79**, 5158 (1997).